PHYSICAL REVIEW C VOLUME 19, NUMBER 5 MAY 1979

Yrast states in ^{52}Fe, ^{52}Mn and the decay of ^{52}Fe^{m}

D. F. Geesaman,* R. L. McGrath, J. W. Noé, and R. E. Malmin†
Department of Physics, State University of New York, Stony Brook, New York 11794
(Received 5 December 1978)

The properties of yrast states of ^{52}Fe and ^{52}Mn were studied using the ^{40}Ca + ^{14}N reaction. In-beam γ-ray singles, γ-γ coincidence, and n-γ coincidence data establish the positions of the lowest 2^+ and 4^+ states of ^{52}Fe as 849.1 ± 0.3 and 2384.6 ± 0.7 keV, respectively. No γ rays associated with other ^{52}Fe states could be found. This is because an ^{52}Fe isomer at 6.83 MeV β^+ decays to ^{52}Mn, diverting strength from the ^{52}Fe γ cascade. Delayed γ-ray singles and γ-γ coincidence data give information on the high-spin yrast states of ^{52}Mn populated in the β^+ decay of the isomer. The results are consistent with several recently published works, and unambiguously establish that the ^{52}Mn 8^+ state is at 2286.0 ± 0.4 keV. The delayed spectra show no indication of direct γ decay of the ^{52}Fe isomer. An upper limit on the γ decay branch is 4×10^{-3}. On the basis of the $(1f_{7/2})^n$ model with "bare" nucleon charges, direct $E4$ γ emission should be the dominant decay mode. It is argued that the absence of $E4$ decay, taken together with known $B(E4)$ data on ^{44}Sc, ^{52}Mn and ^{53}Fe, shows $E4$ effective charges in the $(1f_{7/2})$ shell are different for nuclei located near the beginning or end of the shell. Further, the effective charges near the end of the shell seem to be quite different from those found in $E2$ transitions, i.e., $e_p \sim 0.5$, $e_n \sim -0.5$. First order perturbation calculations in the $(1f,2p)^n$ model offer qualitative, but not quantitative, insight as to the $E4$ effective charge behavior.

RADIOACTIVITY ^{52}Fe^{m}; measured $T_{1/2}$, $\beta\gamma$ coin., β-delayed γ and $\gamma\gamma$ coin.; deduced log ft, $E4$ limit. ^{52}Mn deduced levels.

NUCLEAR REACTIONS ^{40}Ca(^{14}N, np) ^{52}Fe, E = 29 to 38 MeV; measured prompt γ and $n\gamma$ coinc., deduced ^{52}Fe levels.

I. INTRODUCTION

Systematic γ-ray studies with fusion-evaporation reactions have provided extensive information on high-spin states in $f_{7/2}$-shell nuclei. In a number of these nuclei the yrast levels have been established up to the highest spin possible in the $(f_{7/2})^n$ shell-model configuration. This is the case, for example,[1] in the even-even self-conjugate nucleus ^{44}Ti, in which $J_{max} = 12^+$. The yrast level scheme of the cross-conjugate nucleus ^{52}Fe is expected to be similar to that of ^{44}Ti, but prior to the initiation of the present work nothing was known of the ^{52}Fe yrast states with spin $J > 4$. Several transfer-reaction studies of ^{52}Fe had been reported, and in one of these studies[2] the lowest 2^+ and 4^+ states were located to ±30 keV.

In an earlier publication[3] we identified a long-lived isomeric state ($T_{1/2} \cong 50$ s) at 6.8 MeV excitation in ^{52}Fe. The isomer is believed to result from an inversion of the lowest $J^\pi = 10^+$ and 12^+ states, so that the only available decay modes of the 12^+ state are β^+ emission to ^{52}Mn and $E4$ γ-ray decay to the ^{52}Fe 8^+ state. The predominant (>80%) β^+ decay which was observed[3] explains the failure of early attempts[4] to populate low-lying ^{52}Fe levels with fusion-evaporation reactions; the yrast γ-ray cascade terminates at the isomer, and states below the isomer are very weakly populated directly by the fusion-evaporation reaction.

In this paper we report on further studies of the ^{52}Fe yrast states and of the decay modes of the $J^\pi = (12^+)$ isomer. A particular effort was made to find the isomeric $E4$ γ decay which, according to shell-model calculations, should dominate β^+ decay. Two preliminary reports of our experimental results subsequent to the original publication have appeared[5]; a detailed report of this work is given in an unpublished dissertation.[6] Our experimental results are compared to computations based on the $(f_{7/2})^n$ shell model.[7,8] This limited shell-model space seems to provide a reasonable description of many of the properties of $f_{7/2}$-shell high spin states, including the inversion of the yrast 10^+ and 12^+ states in ^{52}Fe.[3,8] Within the framework of the $(f_{7/2})^n$ shell model but considering also more complex configurations, we discuss the systematics of $E4$ transitions in the $f_{7/2}$ shell. It is shown that the effective charges required for $E4$ transitions in this mass region are strikingly different from those appropriate to $E2$ decay.

II. EXPERIMENTAL METHODS

Several different experiments were performed. In each one ^{52}Fe levels were populated with the ^{40}Ca(^{14}N,pn)^{52}Fe fusion-evaporation reaction. Ni-

 © 1979 The American Physical Society

TABLE I. Summary of measurements made on ^{40}Ca + ^{14}N reactions.

Experiment	Target thickness (mg/cm^2)	Incident energy (MeV)
Prompt γ-ray singles	0.3	29, 30, 32, 34, 36, 38
Prompt γ-γ coincidence	0.5	32, 36
Prompt n-γ coincidence	0.5 [a]	30, 32, 34, 36
Delayed γ-ray singles	~2.0	45
Delayed γ-γ coincidence	2.0	45
Delayed β-γ coincidence[b]	0.5	30, 35, 40, 45, 50, 55

[a] ^{40}Ca isotopic enrichment 99.9%; natural calcium was used for the other targets.
[b] This experiment is discussed in Ref. 3.

trogen beams with energies from 29 to 55 MeV were obtained from the Stony Brook FN tandem Van de Graaff accelerator.

In order to identify a possible $E4$ decay branch from the ^{52}Fe isomer it was necessary to obtain a precise energy for a least one of the cascade γ rays which would result. To this end ^{52}Fe yrast transitions were studied in-beam in γ-ray singles, and γ-γ and neutron-γ coincidence experiments. Relatively low bombarding energies of 29 to 38 MeV were employed to favor the direct population of low-spin yrast states below the isomer. In a second set of experiments, delayed γ rays from the decay of ^{52}Fe^{m} were studied in singles and γ-γ coincidence at a somewhat higher energy (45 MeV). Table I summarizes experimental facts about the various measurements. The delayed β-γ coincidence excitation function measurement was done essentially as described earlier[3] and is not discussed further here.

Calcium metal targets 0.3 to 2.0 mg/cm^2 thick were evaporated on gold or tantalum backings. Natural calcium was used except in the n-γ coincidence experiment where enriched isotope (>99.9% ^{40}Ca) was employed to avoid possible interference from the ^{56}Fe $2_1^+ \rightarrow$ g.s. transition (which has nearly the same energy as the corresponding transition in ^{52}Fe). Targets were changed at frequent intervals to minimize the buildup of long-lived activities. Targets used for in-beam experiments were mounted 45° to the incident beam in a small glass chamber.

γ rays were observed in large-volume Ge(Li) detectors with efficiencies of 10–15% relative to standard NaI detectors. The γ-ray detectors used for in-beam measurements were placed at 90° to the incident beam. Usually a graded absorber of a few mm Pb and brass was employed to reduce the flux of low-energy (<500 keV) γ rays. Absolute detector efficiencies were obtained by recording γ rays from various radioactive sources placed at the target position. Energy calibrations were obtained from these sources and known γ-ray lines in the spectra.

In the n-γ coincidence experiment neutrons were detected in a 23 cm diameter by 5 cm thick NE213 liquid scintillator placed at 0° to the incident beam behind a 1.3 cm thick lead γ-ray absorber. Neutron and photon interactions in the detector were distinguished by both pulse-shape analysis and time-of-flight analysis. For each event, pulses corresponding to liquid scintillator pulse-shape, relative interaction time, and γ-ray energy were digitized and written event-by-event on magnetic tape under the control of a PDP-9 computer. The tapes were later analyzed using the same computer by setting gates on various combinations of the parameters. Similar event-mode recording techniques were used in the γ-γ coincidence experiments. In the delayed activity γ-γ coincidence ex-

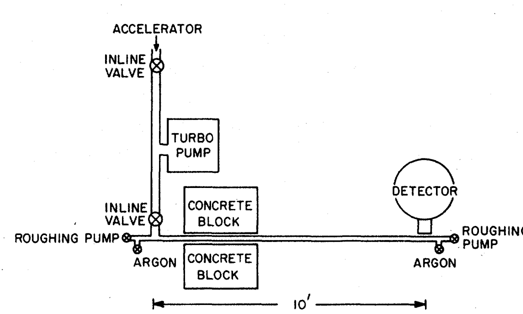

FIG. 1. The pneumatic rabbit system used for delayed activity measurements. A plastic rabbit is transported 10 ft through a stainless steel tube between the irradiation and detector stations. A blast of argon gas followed by roughing pump action is used to achieve transport times ~0.5 s. Sequencing of all valve operations is accomplished with a programmable electronic sequencer.

periment a fourth parameter was the event time relative to the start of the counting interval. This information was obtained by digitizing the output of a linear ramp generator.

In the delayed-activity experiments the target was transported between the irradiation position and a remote counting station by the pneumatic "rabbit" system illustrated in Fig. 1. The sequencing of the various steps in the irradiate-count cycle was controlled by a 10-channel digital programmer unit similar to that described by Schwender, Goosman, and Jones.[9]

The delayed γ-ray singles counting rate (~5000 c/s) precluded event-mode recording. Instead, a multiscaling program was used which recorded on magnetic tape a 4096-channel Ge(Li) spectrum accumulated in the computer memory for 15 s intervals. The duration of the counting interval and the 0.5 s pause for "dumping" were controlled by the PDP-9 60 Hz clock. After eight such 15.5 s count-dump cycles the computer paused while the target was irradiated again under the control of the digital programmer unit. Following the experiment, separate spectra corresponding to each of the eight 15 s time bins were recovered from the tapes. An average system dead-time correction for each time bin was obtained from the integrated counts in a pulser peak placed at the high-energy end of the spectrum.

III. DATA ANALYSIS AND RESULTS

A. Low-lying yrast states in ^{52}Fe

Prior to this work the ^{52}Fe lowest 2^+ and 4^+ states had been located to ±30 keV at 0.84 and 2.36 MeV, respectively, using the ^{54}Fe$(p,t)^{52}$Fe reaction.[2] The only 6^+ state reported was the 5.65 MeV 6^+, $T=1$ analog of the ^{52}Mn ground state. (Comparison with the known[1] level scheme of ^{44}Ti suggests the $T=0$ 6^+ state must be ~1 MeV lower in energy.)

As already discussed, one goal of the present work was to extend knowledge of the ^{52}Fe level scheme. Presumably, the absence of identifiable ^{52}Fe transitions in earlier ^{39}K + ^{16}O and ^{40}Ca + ^{14}N fusion reaction studies[4] is because the ^{52}Fe isomer acts as a "yrast trap" syphoning strength from transitions between lower-lying states.

In the present work a small peak at 849 keV was found in γ-ray singles spectra from the ^{40}Ca + ^{14}N reaction at bombarding energies near the Coulomb barrier. This γ ray was demonstrated to come from the ^{52}Fe $2^+ \to$ g.s. transition. Prompt γ-ray singles spectra were obtained at incident ^{14}N energies from 29 to 38 MeV (see Table I). Figure 2 shows some excitation functions measured for the first-excited state to g.s. transitions in ^{51,52}Mn

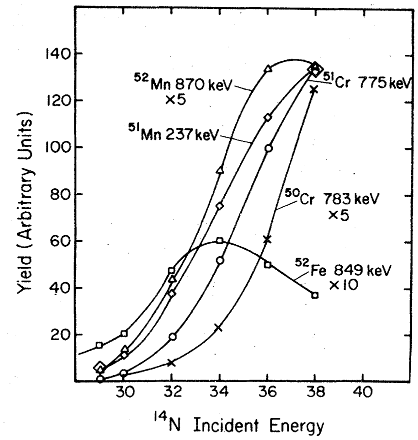

FIG. 2. Excitation functions for some prompt γ rays from ^{40}Ca + ^{14}N reactions. These γ rays are from low-lying state to g.s. transitions.

and ^{50,51}Cr (Refs. 10–15), and for the 849 keV γ ray. The yield of this γ ray peaks at ~34 MeV. That this energy is somewhat lower than the peak energy for ^{52}Mn production (~37 MeV) or ^{52}Fe isomer production (~39 MeV—see below) is probably because of isomer trapping. The origin of the 849 keV γ ray was tested by comparing its yield to the ^{52}Fe g.s. yield over the full range of bombarding energies. After each in-beam yield measurement the production cross section for the 9.3 h ^{52}Fe g.s. activity was obtained by counting the associated 169 keV γ rays.[16] Within errors (about 20%) the measured cross section ratio σ(849 keV γ ray)/σ(^{52}Fe g.s.) was 1.6 *and constant* over the whole range of bombarding energies. This result is taken as strong evidence that the 849 keV γ ray is associated with the ^{52}Fe $2^+ \to$ g.s. transition since

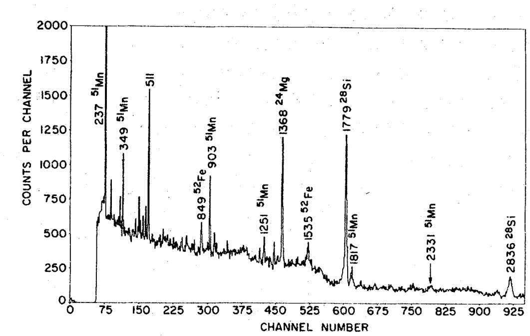

FIG. 3. Spectrum of prompt γ rays in coincidence with neutrons. Neutron gating relatively enhances γ rays associated with the $2p,n$ (^{51}Mn) and p,n (^{52}Fe) reactions. The ^{24}Mg and ^{28}Si γ rays are due to ^{12}C and ^{16}O target contamination.

TABLE II. Energies of γ rays in ^{52}Fe and ^{52}Mn.

	Avrigeanu *et al.* [a]	Stefanini *et al.* [b]	Evers *et al.* [c]	Iritani [d]	Present work
^{52}Fe					
$4^+ \to 2^+$	...	...	1535.0 ± 0.9	1536.0 ± 0.7	1535.2 ± 0.8
$2^+ \to 0^+$	849.0 ± 1.5	...	848.3 ± 0.9	849.5 ± 0.7	849.1 ± 0.4
^{52}Mn					
$11^+ \to 9^+$	929.0 ± 0.4	928.7 ± 1.0	929.7 ± 0.3	...	929.5 ± 0.2
$9^+ \to 8^+$	621.8 ± 0.4	621.5 ± 0.7	621.6 ± 0.2	...	621.7 ± 0.2
$9^+ \to 7^+$	2037.5 ± 1.0	2038.25 ± 0.7	2037.5 ± 0.3	...	2037.6 ± 0.4
$8^+ \to 7^+$	1415.5 ± 0.4	1416.4 ± 0.7	1416.0 ± 0.2	...	1416.1 ± 0.2
$8^+ \to 6^+$	2286 ± 2	2285.8 ± 0.7	2285.6 (no error)	...	2285.9 ± 0.4
$7^+ \to 6^+$	869.4 ± 0.5	869.4 ± 0.35	869.5 ± 0.3	...	869.9 ± 0.2
$10^+ \to 9^+$	...	...	1256.5 ± 0.3	...	...

[a] Reference 12.
[b] Reference 13.
[c] Reference 17.
[d] Reference 18.

the production cross sections for *different* nuclides have differing incident energy dependence (Fig. 2).

The ^{40}Ca + ^{14}N γ-ray singles spectra are relatively complex because of competing p, n, and α evaporation. Neutron gating simplifies the spectra so that ^{52}Fe transitions (produced via n,p evaporation) are relatively enhanced. The n-γ coincidence γ-ray spectrum in Fig. 3 shows the ^{52}Fe 849 keV γ ray, as well as peaks from known[10] ^{51}Mn transitions (produced via $2p, n$ evaporation) and from target contaminant reactions.

The 1535 keV γ ray evident in Fig. 3 comes from the ^{52}Fe $4^+ \to 2^+$ transition. This was established in a separate γ-γ coincidence measurement which showed the 849 and 1535 keV γ rays are coincident. Unfortunately, these data showed no evidence for other γ rays in the range 200 to 3000 keV which might come from other ^{52}Fe transitions. However, the statistics were poor enough that a transition with up to 50% of the yield of the $4^+ \to 2^+$ transition might have been obscured.

Table II summarizes present results on the yrast transitions in ^{52}Fe. Other recent results from several ^{39}K(^{16}O,$p2n$), ^{50}Cr($\alpha,2n$), and ^{50}Cr(^{3}He,n) reactions[12,17,18] are also given. The weighted averages show the ^{52}Fe 2^+ and 4^+ states exist at 849.1 ± 0.3 and 2384.6 ± 0.7 keV, respectively.

B. Delayed activities: The ^{52}Mn level scheme and decay properties of ^{52}Fe^m

The existence of the ^{52}Fe isomeric state was discovered by finding five delayed γ rays associated with ^{52}Mn transitions in coincidence with β^+ particles.[3] The half-life and β^+ end point associated with each γ ray were the same within error, indicating the isomer β^+ decayed exclusively to the highest ^{52}Mn state associated with the γ-ray cascade. To complement the original β-γ coincidence data, delayed γ-ray singles, and γ-γ coincidence data have been obtained in order to confirm the decay scheme of the ^{52}Fe isomer, and

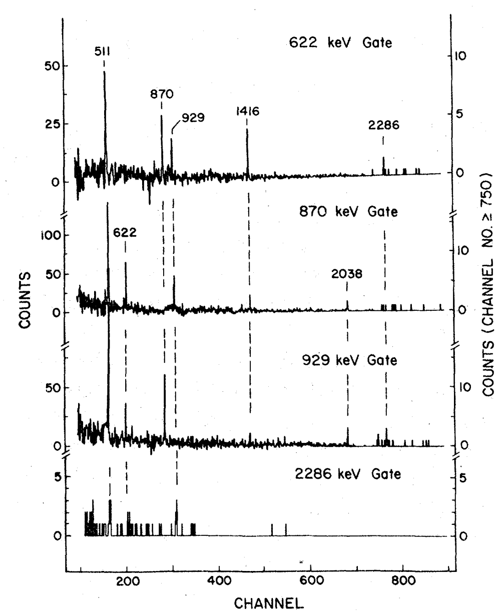

FIG. 4. Delayed γ-γ coincidence data. The spectra show γ rays coincident with four γ rays in the ^{52}Mn high-spin decay scheme. A weak 2286 keV γ ray in the 622 and 929 keV gated spectra shows that the ^{52}Mn 8^+ state is at 2286 keV. These data establish the ^{52}Mn decay scheme shown in Fig. 5. The vertical scale is expanded for channel numbers > 750.

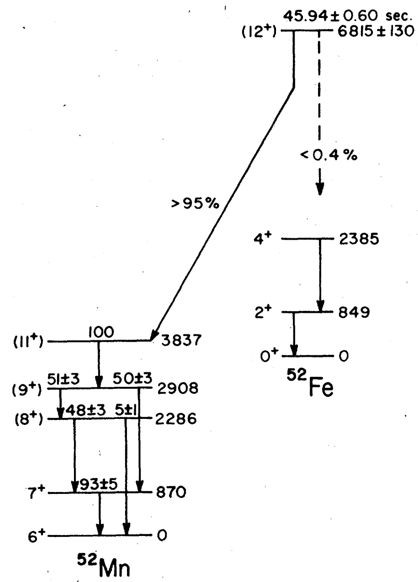

FIG. 5. Levels and decay schemes of ^{52}Fe and ^{52}Mn found in the present work. In ^{52}Mn the γ-ray intensities are given relative to the $11^+ \rightarrow 9^+$ transition. Intensities were obtained from delayed γ-ray singles data.

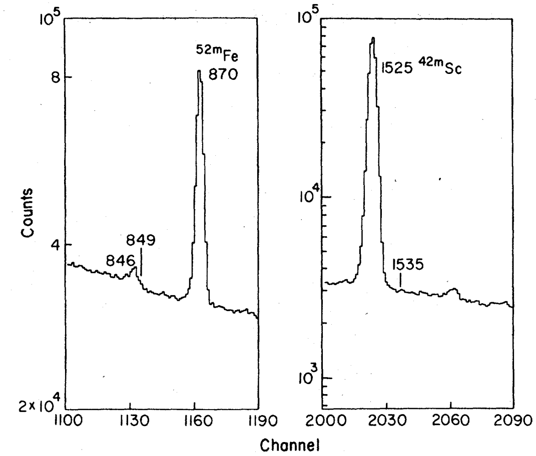

FIG. 7. Delayed γ-ray singles spectra in the energy regions encompassing the ^{52}Fe $2^+ \rightarrow$ g.s. and $4^+ \rightarrow 2^+$ transitions at 849 and 1535 keV, respectively. The absence of observable γ ray peaks at these energies provides an upper limit on direct $E4$ γ-decay branch of ^{52}Fe^m.

to search for a direct γ-ray decay branch. These data also establish a revised level scheme for ^{52}Mn.

Spectra of γ rays in coincidence with four delayed γ rays from ^{52}Mn are shown in Fig. 4. A previously unreported weak 2286 keV γ-ray is in coincidence with the 929 and 622 keV γ rays. The ^{52}Mn level scheme shown in Fig. 5 is constructed on the basis of these coincidence spectra together with the delayed γ-ray singles data. The ^{52}Mn spin-parity assignments are taken from Avrigeanu *et al.*[12] and from Stefanini *et al.*[13] Our coincidence data confirm that the ^{52}Mn 8^+ state is at 2286 keV. (Originally this state had been placed at 1492 keV, with the ordering of the 622 and 1416 keV transitions reversed—see Ref. 3.) Other recently published papers, citing our preliminary results, have reported the same level scheme using less direct methods.[12,13,17] The γ-ray energies

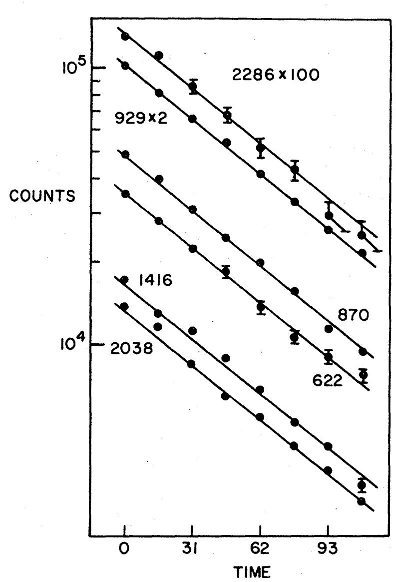

FIG. 6. Decay rates of the six γ rays in the ^{52}Mn high-spin decay scheme. The γ-ray singles data were obtained with the rabbit system shown in Fig. 1.

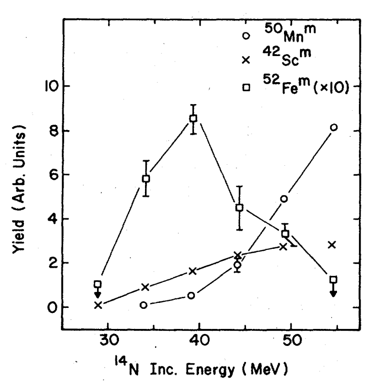

FIG. 8. Excitation functions for some delayed γ-ray activities from ^{40}Ca+^{14}N reactions.

from these papers are compared with the present results in Table II. Except for the six γ rays from transitions shown in Fig. 5, no other γ rays with energies between 0.52 and 3.0 MeV were observed with the required $^{52}Fe^m$ half-life which could account for more than a 5% decay branch.

A weighted average of the half-lives of each of these γ rays gives 45.9 ± 0.6 s for the half-life of $^{52}Fe^m$. The decay rates of these γ rays are shown in Fig. 6. To check the accuracy of our procedures, the half-lives of $^{42}Sc^m$ and ^{50}Mn were determined from the same data set to be 61.9 ± 0.7 and 104.5 ± 1.3 s, respectively. These agree with published values 62.0 ± 0.3 (Ref. 19) and 105.6 ± 1.8 s.[20] The half-life of $^{52}Fe^m$, and the β^+ end point energy 4.33 ± 0.13 MeV (Refs. 3 and 6) give $\log ft = 4.83 \pm 0.11$ for the isomer β decay. The properties of ^{52}Fe found here are illustrated in Fig. 5.

Armed with the precise excitation energies of the ^{52}Fe yrast 2^+ and 4^+ states found from the in-beam analysis, it was possible to hunt for evidence of direct γ decay of $^{52}Fe^m$ in the delayed γ-ray singles data. (Any direct γ decay is expected to cascade through the yrast states.) Portions of the delayed γ-ray spectra in the energy regions encompassing the $2^+ \to$ g.s. and $4^+ \to 2^+$ transitions are shown in Fig. 7. An 849 keV γ ray would lie on the upper side of the peak labeled 846. (Activity from ^{56}Co, ^{27}Mg, or other nuclides could produce this peak.) Using a standard line shape obtained from the 870 keV γ ray, an upper limit of 2×10^{-2} (2σ limit) can be set on the yield of an 849 keV γ ray relative to the 870 keV γ - ray yield. An even lower limit can be obtained from the region where a 1535 keV γ ray would appear since the spectrum is structureless here. After correcting for relative efficiencies, an upper limit of the ratio of the yields of a 1535 keV γ ray to the 870 keV γ ray is 4×10^{-3} (2σ limit). Thus, the direct $E4$ γ-decay branching ratio of $^{52}Fe^m$ is $\leq 4 \times 10^{-3}$.

It is interesting to contrast the excitation functions of the delayed $^{52}Fe^m$ activity which is shown in Fig. 8 (along with the other relatively short-lived activities of ^{50}Mn and $^{42}Sc^m$) and the prompt activities shown in Fig. 2. Because $^{52}Fe^m$ diverts the yrast cascade to ^{52}Mn, the ^{52}Fe $2^+ \to$ g.s. γ-ray yields falls as the $^{52}Fe^m$ activity yield rises.

IV. DISCUSSION

The existence of long-lived "spin-gap" isomers in ^{211}Po, ^{212}Po,[21] and ^{93}Mo (Ref. 22) has been known for some time. The isomers are believed to be simple three or four particle shell-model states.[23] The structure of the isomers in ^{53}Fe[24] and in ^{52}Fe is similar. In each case, the isomeric state is a "stretched" configuration where the nucleons are coupled to the maximum possible spin. For example, the ^{52}Fe isomer is described as four $1f_{7/2}$ holes in the ^{56}Ni core coupled to spin 12: $|(\nu f_{7/2})_6^{-2} \otimes (\pi f_{7/2})_6^{-2}; J=12\rangle$. For this highly aligned state, the spatial overlap of the nucleonic wave functions is larger than that in any configuration of comparable spin. Short range attractive residual interactions can cause increased binding for the maximally aligned state. This phenomena is, of course, reflected in typical two-body interactions which are most attractive for states of minimum and maximum total angular momentum.[25] At present, there is speculation that this effect may produce isomers at very high excitations and spins.[26]

In several-particle or -hole states, isomer existence is determined by a precarious balance between the increasingly attractive two-body $T=0$ interactions and the decreasingly attractive $T=1$ interactions as a function of increased two-body angular momentum. Thus it is likely that these isomers exist only near closed shells, since the number of $T=1$ interactions increases faster than the number of $T=0$ interactions when particles or holes are added to closed shells.

We have done calculations in the $1f_{7/2}$ model space with two purposes in mind. First, the influence of particular choices of two-body residual interactions on the predicted existence of isomers was investigated. Next, the decay properties of $^{52}Fe^m$ were computed for comparison with the observed properties. Subsequently perturbation calculations involving admixtures in the $1f_{5/2}$, $2p_{3/2}$ shells were done to see whether better results could be obtained.

When calculations involve only one shell, the calculated spectra of particle-hole conjugate nuclei are identical for a given two-body interaction.[7] In $1f_{7/2}$ shell nuclei the spectra of conjugates are indeed similar. However, symmetry breaking effects exist. For example, the angular momenta of the yrast levels in ^{44}Ti and ^{43}Sc have the normal monotonic dependence on energy, but the conjugates, ^{52}Fe and ^{53}Fe, each have an isomeric level. Thus a single two-body residual interaction cannot reproduce the spectra at both ends of the shell. A "fall-back" position is to use two different sets of empirical effective interactions taken from appropriate ends of the shell. This was tried. The interactions were obtained from the experimental spectra of ^{42}Sc (Ref. 27) and ^{54}Co (Ref. 28) which were assumed to give the $(1f_{7/2})^2$ and $(1f_{7/2})^{-2}$ interaction energies, respectively. The resulting four particle-hole and three particle-hole spectra are in good agreement with experiment as shown in Figs. 9 and 10. The experimental spectra are

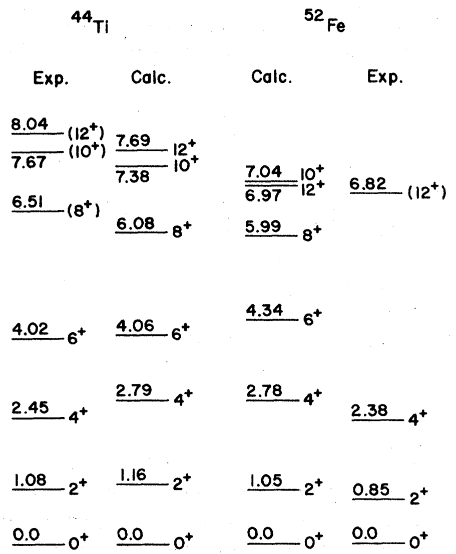

FIG. 9. Comparison of experimental and $(1f_{7/2})^{\pm 4}$ model level schemes of ^{44}Ti and ^{52}Fe. Two different empirical effective interactions taken from ^{42}Sc and ^{54}Co spectra were used for ^{44}Ti and ^{52}Fe, respectively.

taken from Ref. 1 (^{44}Ti), Ref. 29 (^{43}Sc), and Ref. 30 (^{53}Fe). Evidently a unified description of nuclei spanning the $1f_{7/2}$ shell region requires a larger shell-model basis. However, the "local" success of these calculations may indicate that the major influence of other shell-model orbitals is a gradual renormalization of the $1f_{7/2}$ quasiparticle.

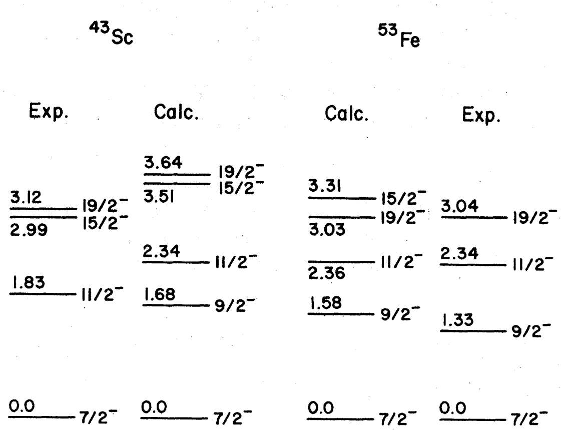

FIG. 10. Comparison of experimental and $(1f_{7/2})^{\pm 3}$ model level schemes of ^{43}Sc and ^{53}Fe. Effective interactions taken from ^{42}Sc and ^{54}Co spectra were used for ^{43}Sc and ^{53}Fe, respectively.

It is well known that large renormalizations of single-particle operators are required to reproduce experimental transition matrix elements within the $(1f_{7/2})^n$ model space.[7] This also happens with the β and $E4$ matrix elements relevant to the present work. For example, assuming pure $(1f_{7/2})$ structure, the calculated logft value for the ^{52}Fe 12^+ to ^{52}Mn 11^+ β^+ decay is only 3.93, compared to the observed 4.83 ± 0.11. Since β-decay rates in this mass region are quite sensitive to $1f_{5/2}$ admixtures, sufficient retardation to account for the experimental rate is readily obtained with a first order perturbation theory calculation as discussed below.

An apparently striking discrepancy between $(1f_{7/2})^n$ calculations and experiment exists with the ^{52}Fe $12^+ \to 8^+$ $E4$ γ decay rate. Using bare nucleon charges, harmonic oscillator single-particle states ($\hbar\omega = 41\ A^{-1/3}$ MeV), and the computed $12^+ \to 8^+$ state energy separation 976 keV (see Fig. 9), the $E4$ lifetime is expected to be 6 s. Hence, the direct $E4$ decay mode ought to dominate over β^+ decay rather than be a very weak branch ($\leq 4 \times 10^{-3}$). Clearly, because the $E4$ lifetime is proportional to the ninth power of the energy separation between the 12^+ and 8^+ states, it is crucial to know the actual excitation energies of these states. Nonetheless it seems likely to us that the $E4$ rate is indeed much slower than expected in the $(1f_{7/2})^n$ model. The *actual* energy separation of these states would have to be less than 370 keV to bring the $(1f_{7/2})^n$ model $E4$ lifetime into line with experiment. It is unlikely that the model prediction is this much in error, since the model reproduces the yrast levels of ^{53}Fe quite reliably, with a root-mean-square deviation of only 120 keV. A retarded ^{52}Fe^m $B(E4)$ transition rate places severe constraints on the $E4$ effective charge in this mass region. $B(E4)$ values have been measured in two neighboring nuclei, ^{52}Mn (Ref. 31) and ^{53}Fe.[32] In both cases the observed $B(E4)$ values are smaller than predicted with the $(1f_{7/2})^n$ model with bare nucleon charges, as indicated in Table III.

These $B(E4)$ values require $e_p \approx 0.5$ and are relatively insensitive to e_n (see Table III). The ^{52}Fe $12^+ \to 8^+$ $B(E4)$ is proportional to $(e_p + e_n)^2$ because both states have $T=0$. Clearly, the $B(E4)$ vanishes if $e_n = -0.5$. This, of course, implies an isoscalar polarization charge $\delta e_{\rm pol} = -0.5$ where $e_p = 1 + \delta e_{\rm pol}$ and $e_n = \delta e_{\rm pol}$.

One other $B(E4)$ is known in the $1f_{7/2}$ shell in ^{44}Sc.[33] This is larger than the $(1f_{7/2})^n$ model prediction, requiring $e_n \approx 1.4$ and is relatively insensitive to e_p (see Table III). Obviously, because this charge is radically different from the charge at the upper end of the $1f_{7/2}$ shell, the assumption

TABLE III. $E4$ γ transitions in the $1f_{7/2}$ shell. Experimental $B(E4)$'s are compared to the Weisskopf unit (W.u.) and to formulas obtained from the $(1f_{7/2})^n$ shell model. e_p and e_n are proton and neutron effective charges. $e_p = 1 + \delta e_{pol}$ and $e_n = \delta e_{pol}$, where δe_{pol} is the isoscalar polarization charge.

Nucleus	Exp. $B(E4)$ (e^2 fm^8)	W.u. (e^2 fm^8)	Exp./W.u.	$(1f_{7/2})^n$ model (e^2 fm^8)	δe_{pol}
^{44}Sc	1.9×10^3	1.5×10^3	1.2	$(5.98e_p + 27.23e_n)^2$	1.1
^{52}Mn	3.3×10^2	2.4×10^3	0.14	$(48.9e_p + 7.8e_n)^2$	−0.53
^{53}Fe	6.5×10^2	2.5×10^3	0.26	$(49.1e_p + 4.2e_n)^2$	−0.44
^{52}Fe [a]	≤ 0.36	2.4×10^3	$\leq 2\times10^{-4}$	$(29.3e_p + 29.3e_n)^2$	$-0.51 \leq \delta e \leq -0.49$

[a] The energy separation of the 12^+ and 8^+ states is taken to be 976 keV as calculated in the $(1f_{7/2})^n$ shell model as discussed in the text.

that the polarization charge is isoscalar is suspect. Dropping this assumption, all three *measured* $B(E4)$ values can roughly be fitted with a single set of effective charges. The ^{52}Mn and ^{53}Fe^m transition rates require $e_p \approx 0.3$, while the ^{44}Sc transition rate requires $e_n \approx 1.5$. However, these values lead to an *enhanced* $B(E4)$ value for ^{52}Fe since $(e_p + e_n)^2 \approx 3$, which tentatively seems to disagree with experiment. Thus it appears that different $E4$ polarization charges are required to fit transition rates of nuclei near the lower and upper ends of the $1f_{7/2}$ shell.

It is interesting that the $B(E6)$ value measured[30] for ^{53}Fe^m also requires $e_p \approx 0.5$. Electron scattering data[34] indicate that $B(E6)$ values in ^{50,52}Cr are also reduced compared to bare nucleon charge predictions. This raises the possibility that $E4$ and $E6$ polarization charges are comparable, arising from a similar mechanism. Certainly the polarization charges deduced from high multipole transitions are very different from those found for $E2$ transitions ($\delta e_{pol} \sim 0.9$) in the $(1f_{7/2})^n$ model.[35]

The renormalization effects which are "lumped" into an empirically determined effective charge are, of course, microscopically quite complicated. One important contribution to the $E4$ polarization charge is the admixture of other orbitals of the (fp) major oscillator shell into the $f^n_{7/2}$ states. These contributions were estimated by including $p_{3/2}$ and $f_{5/2}$ admixtures with first order perturbation theory. Kuo and Brown effective matrix elements[36] were used throughout the calculation along with several sets of single-particle energies. Zeroth order wave functions were taken from a diagonalization of the $f^n_{7/2}$ model space. Results with the set of single-particle energies originally used by Kuo-Brown are shown in Table IV.

The modifications to the $(1f_{7/2})^n$ model predictions improve agreement with experiment. The results also suggest the $E4$ polarization charge changes sign as the shell fills. The magnitude of the perturbation effects is not large enough to account for the entire empirical $f_{7/2}$ charge, so that sizable polarization charges are still required to reproduce the experimental transition rates. However, because these calculations were done only to indicate trends, we find the results quite encouraging. The same perturbation calculation gives $\log ft = 5.41$ for the isomeric 12^+ to 11^+ transition. Thus, these parameters actually retard the β^+-decay rate, which is very sensitive to $1f_{5/2}$ admixtures, too much.

A similar treatment of the ^{53}Fe^m $E6$ decay rate has been reported by Gloeckner and Lawson.[37]

TABLE IV. $(1f_{7/2})^n$ and $(1f, 2p)^n$-model predictions of $[B(E4)]^{1/2}$. Calculations in the (fp) space were done in first order perturbation approximation using Kuo-Brown matrix elements and the single particle energies $E(1f_{7/2}) = 0$, $E(2p_{3/2}) = 2.1$ MeV, and $E(1f_{5/2}) = 6.5$ MeV. [a] All units are $e$fm^4. δe_{pol} is defined in Table III.

Nucleus	$(1f_{7/2})^n$ model [b]	δe_{pol}	$(1f, 2p)^n$ model	δe_{pol}	Exp. $\sqrt{B(E4)}$
^{44}Sc	$4.5e_p + 26.9e_n$	1.2	$8.1e_p + 38.9e_n$	0.8	43.6
^{53}Fe	$40.1e_p + 4.2e_n$	−0.4	$40.3e_p + 13.2e_n$	−0.3	25.5
^{52}Fe	$29.3e_p + 29.3e_n$	−0.5	$15.0e_p + 15.0e_n$	−0.5	≤0.6

[a] Reference 36.

[b] The differences between these values and those in Table III are caused by the different $(1f_{7/2})^2$ two-body matrix elements.

They find that $f_{5/2}$ admixtures ($p_{3/2}$ admixtures cannot contribute to the $B(E6)$ in first order) reduce the calculated $^{53}Fe^m$ $B(E6)$ value toward the experimental value. The magnitude of the correction is comparable to what we obtain for the $^{53}Fe^m$ $B(E4)$.

Several other configuration admixtures could be important in $E4$ transitions. Horikawa *et al.*[38] have investigated the effects of changing one particle by two or more major oscillator shells. They obtain effective charges of $e_p = 1.05$ and $e_n = 0.29$ from this mechanism, and conclude that abnormally strong $T=1$ $S=1$ central or spin-orbit interactions would be necessary to obtain the large change in the proton effective charge required for the $^{53}Fe^m$ and ^{52}Mn $B(E4)$'s. Such abnormally strong interactions would not be compatible with the free nucleon-nucleon interaction nor with the effective charges of lower multipoles. Another type of contribution to the $E4$ matrix element might arise from the excitation of two particles from the (sd) shell to the (fp) shell or from the (fp) shell to the next higher oscillator shell. Since this is a second order effect it is much harder to estimate. Calculations[39] indicate that such admixtures may account for the state dependence of the $E2$ effective charges in ^{42}Ca. Since little state dependence is observed[40] in the $E2$ effective charges in ^{46}Ca and ^{54}Fe, these configurations may be less important in the middle of the (fp) shell. If such an effect were localized around ^{40}Ca, it might account for the large $E4$ matrix element of ^{44}Sc.

V. CONCLUSIONS

In this paper we have reported on further studies of the ^{52}Fe 6.8 MeV isomeric state as well as the low-lying levels of ^{52}Fe. The more precise value of 45.9 ± 0.6 s has been obtained for the half-life of the isomeric state. No additional[3] decay branches were observed. The very low upper limit we have set on the branching ratio for direct γ decay of the isomer is particularly interesting. The *tentative*, model dependent $B(E4)$ upper limit for $^{52}Fe^m$, along with the previously measured $B(E4)$ values for ^{52}Mn and $^{53}Fe^m$ suggests that the $E4$ effective charges of the neutron and proton are approximately equal and opposite in sign in this mass region. Additionally, the polarization charge apparently changes sign from the beginning to the end of the $f_{7/2}$ shell. Quite different effective charges are required for $E2$ transitions.

We are encouraged by the qualitative agreement between perturbation theory calculations and experiment which suggests the polarization charge changes sign from one end of the shell to the other. However, more elaborate calculations are required to achieve quantitative success. It will be interesting to see whether high order electromagnetic transition systematics in other mass regions exhibit similar effective charge behavior.

A measurement of the position of the 8^+ yrast state of ^{52}Fe is a prerequisite to establishing a model-independent $B(E4)$ upper limit. Unfortunately, the decay properties of $^{52}Fe^m$ make this arduous—as is clear from the present work.

We thank D. Strottman, A. Arima, and R. Lawson for stimulating discussions about $E4$ transitions. We are indebted to Professor R. Sherr for giving us unpublished data on ^{54}Co. We thank P. Gural for assistance in collecting and analyzing the data. This research was supported in part by the National Science Foundation.

---

*Present address: Physics Division, Argonne National Laboratory, Argonne, Illinois.

†Present address: Physics Department, Notre Dame University, South Bend, Indiana.

[1]J. J. Kolata, J. W. Olness, and E. K. Warburton, Phys. Rev. C 10, 1663 (1974).

[2]J. B. Viano, Y. Dupont, and J. Menet, Phys. Lett. 34B, 397 (1971).

[3]D. F. Geesaman, R. E. Malmin, R. L. McGrath, J. W. Noé, and J. Cerny, Phys. Rev. Lett. 34, 326 (1975).

[4]J. J. Kolata, private communication; J. W. Noé, R. W. Zurmühle, and D. P. Balamuth (unpublished).

[5]D. F. Geesaman, J. W. Noé, R. E. Malmin, and R. L. McGrath, Bull. Am. Phys. Soc. 21, 83 (1976); D. F. Geesaman, R. E. Malmin, R. L. McGrath, and J. W. Noé, in Proceedings of the Topical Conference on Physics of Medium-Light Nuclei, Florence, 1977 (Editrice Compositori, Bologna, 1978).

[6]D. F. Geesaman, Ph.D. thesis, SUNY-Stony Brook, 1976 (unpublished).

[7]J. D. McCullen, B. F. Bayman, and L. Zamick, Phys. Rev. 134, B515 (1964).

[8]W. Kutschera, B. A. Brown, and K. Ogawa (unpublished).

[9]G. E. Schwender, D. R. Goosman, and K. W. Jones, Rev. Sci. Instrum. 43, 832 (1972).

[10]J. W. Noé, R. W. Zurmühle, and D. P. Balamuth, Nucl. Phys. A277, 137 (1977).

[11]J. W. Noé and P. Gural, *Proceedings of the Topical Conference on Physics of Medium-Light Nuclei, Florence, 1977* (Editrice Compositori, Bologna, 1978).

[12]V. Avrigeanu, D. Bucurescu, G. Constantinescu, E. Dragulescu, M. Ivascu, D. Pantelica, and R. Teodorescu, Nucl. Phys. A272, 243 (1976).

[13]A. M. Stefanini, C. Signorini, M. Morando, and R. A. Ricci, Nuovo Cimento 33A, 460 (1976).

[14]W. Kutschera, R. B. Huber, C. Signorini, and H. Morinaga, Phys. Rev. Lett. 33, 1108 (1974).

[15]Z. P. Sawa, J. Blomqvist, and W. Gullholmer, Nucl.

Phys. A205, 2507 (1973).

[16]W. W. Bowman and K. W. MacMurdo, At. Data Nucl. Data Tables 13, 93 (1974).

[17]D. Evers, A. Harasim, R. L. McGrath, and W. Assmann, Phys. Rev. C 15, 1690 (1977).

[18]Y. Iritani, J. Kasagi, and M. Ohnuma, J. Phys. Soc. Japan 43, 1119 (1977).

[19]D. W. Wilkinson and D. E. Alburger, Phys. Rev. C 10, 1993 (1974).

[20]S. Raman, R. L. Auble, W. T. Milner, J. B. Ball, F. K. McGowan, P. H. Stelson, and R. L. Robinson, Nucl. Phys. A184, 138 (1972).

[21]I. Perlman, F. Asaro, A. Ghiorso, A. Larsh, and R. Latimer, Phys. Rev. 127, 917 (1962).

[22]M. Goldhaber and R. D. Hill, Rev. Mod. Phys. 24, 79 (1952).

[23]N. K. Glendenning, Phys. Rev. 127, 923 (1962); N. Auerbach and I. Talmi, Phys. Lett. 10, 297 (1964).

[24]J. Vervier, Nucl. Phys. A103, 222 (1967).

[25]J. D. Schiffer and W. W. True, Rev. Mod. Phys. 48, 191 (1976).

[26]A. Faessler, M. Ploszajczak, and K. R. S. Devi, Phys. Rev. Lett. 36, 1028 (1976).

[27]J. J. Schwartz, D. Cline, H. E. Gove, R. Sherr, T. S. Bhattia, and R. H. Siemssen, Phy. Rev. Lett. 19, 1482 (1967).

[28]The ^{54}Fe(^{3}He, t)^{54}Co reaction, which is expected to populate all $(f_{7/2})^{-2}$states, has been studied by J. J. Schwartz, R. Sherr, and T. Bhattia, Bull. Am. Phys. Soc. 13, 1446 (1968), and R. Sherr, J. J. Schwartz, and T. Bhattia (unpublished). The ^{54}Fe(^{6}Li, ^{6}He)^{54}Co reaction, which strongly populates the $T=0$ $(f_{7/2})^{-2}$ states, has been studied by R. L. McGrath, D. F. Geesaman, L. L. Lee, Jr., J. W. Noé, and C. E. Thorn, Bull. Am. Phys. Soc. 22, 527 (1977), and unpublished. These data, taken together, show that the 0^+, 1^+, 2^+, 4^+, and 7^+ states are at 0.00, 0.94, 1.45, 2.64, and 0.20 MeV, respectively. The data give the tentative locations of the 3^+, 5^+, and 6^+ states as 2.28, 2.15, and 3.08 MeV, respectively. These energies were used in the present calculations.

[29]P. M. Endt and C. van der Leun; Nucl. Phys. A214, 1 (1973).

[30]J. N. Black, William C. McHarris, W. H. Kelly, and B. H. Wildenthal, Phys. Rev. C 11, 939 (1975).

[31]A. Pakkanen, Ann. Acad. Sci. Fenn. A253, 8 (1967).

[32]K. Eskola, Phys. Lett. 23, 471 (1966).

[33]H. K. Walter, A. Weitsch, and H. J. Welke, Z. Phys. 213, 323 (1968).

[34]J. W. Lightbody, Jr., J. B. Bellicard, P. de Witt-Hubert, B. Frois, Phan Xuan Ho, P. Leconte, A. Nakada, and S. Turek, Bull. Am. Phys. Soc. 20, 568 (1975).

[35]B. A. Brown, D. B. Fossan, J. M. McDonald, and K. A. Snover, Phys. Rev. C 9, 1033 (1974).

[36]T. T. S. Kuo and G. E. Brown, Nucl. Phys. A114, 241 (1968).

[37]D. H. Gloeckner and R. D. Lawson, Phys. Rev. C 11, 1832 (1975).

[38]Y. Horikawa, T. Hoshino, and A. Arima, Phys. Lett. 63B, 134 (1976).

[39]B. H. Flowers and L. D. Skouras, Nucl. Phys. A136, 35 (1969).

[40]W. Kutschera, B. A. Brown, H. Ikezoe, G. D. Sprouse, Y. Yamazaki, Y. Yoshida, T. Namura, and H. Ohnuma, Phys. Rev. C 12, 813 (1975), and references therein.